*

Photovoltaic and Battery Systems Sizing Optimization for Ultra-Fast Charging Station Integration

Carola Leone, Carlo Peretti, Andrea Paris, and Michela Longo
Politecnico di Milano, Energy Department
Milan, 20056, Italy

***Abstract*—The installation of Ultra-Fast Charging stations (UFCS) is of vital importance to enhance and support the global shift to electric mobility. However, since UFCSs require a huge amount of energy in short period of time, their integration with the energy transmission and distribution grids will lead to a considerable number of technical challenges. To mitigate these negative aspects the incorporation of a Photovoltaic (PV) power plant and a Battery Energy Storage System (BESS) in the station systems seems crucial. In this paper an optimization study to find the size of these additional components is carried out. The final aim is to find their optimal dimensions to make the integration the most convenient as possible from an economic point of view. To achieve such a purpose, a single-objective optimization problem is simulated. The objective function aims to maximize the Net Present Value (NPV) of the overall charging station. The single-objective function is optimized through a genetic algorithm (GA) and the optimization toolbox embedded in the MATLAB software has been used to run the proposed optimization. The results highlight how the configuration complemented with the PV plant and the BESS is better from a technical-economic perspective. As a matter of fact, the profitability of such UFCS will be 7.5% higher than the solution without additional components.**

***Index Terms*— Electric Mobility, Ultra-Fast charging station, Photovoltaic, Battery storage systems, Extreme charging.**

I. Introduction

TRANSPORT represents almost a quarter of Europe's greenhouse gas emissions and is the main cause of air pollution in cities [1]. Figure 1 shows the trend of carbon dioxide CO_2 emission for different sectors in Europe. As can be seen, starting from 1990, the only sector with a strong increase (until 2007) is the transportation one. The reduction of greenhouse gases emission in this sector could be reached only with a robust and quick switch to EVs (Electric Vehicles) [1]-[2]. The electrification trend has started few years ago and it is having an important growth due to the decarbonization policies of the European Union and its vehicle manufacturers. Therefore, the penetration of EVs is expected to grow exponentially over the next few years. To promote and support this electrification trend the installation of consistent and well-integrated charging infrastructure is required.

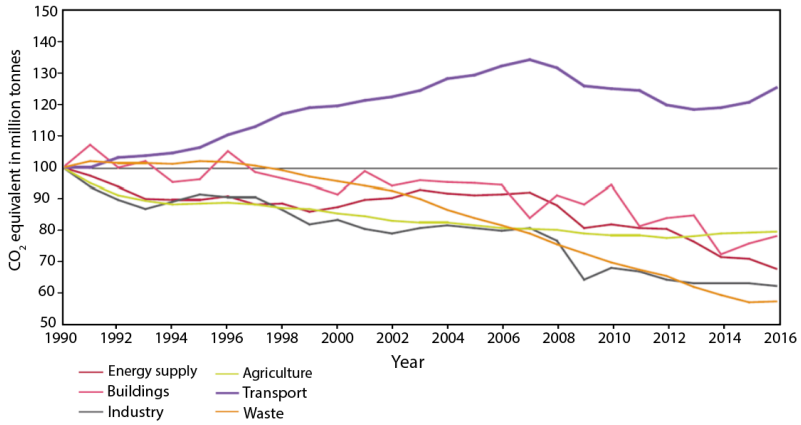

*Corresponding author: Carola Leone.

The authors are with the Department of Energy, Politecnico di Milano, Milano 20133, Italy (e-mail: carola.leone@polimi.it; carlo1.peretti@mail.polimi.it; andrea.paris@mail.polimi.it; michela.longo@polimi.it).

Figure 1 Sectors emissions relative trends with respect to 1990.

In Italy, the number of publicly accessible AC charging points available in the country increased exponentially over the last five years, passing from 1,679 units in 2015 to 12,150 units in 2020 [3]. Nevertheless, these numbers do not take into account the extreme fast-charging systems, which become essential when medium and long-distance travels are concerned. Ultra-fast or extreme charging (UFC) systems have typical power rates between 50 kW up to 350 kW [4]. Therefore, compared to slow charging, UFC allows recharging the EV in about 25-35 minutes. However, its biggest disadvantage is that of requiring large power demand, and hence, greatly impact on the national electric grid [5]. Indeed, the power demand of such an infrastructure is a new load for the grid characterized by a random fluctuating behavior and high peak power density for short periods [6].To tackle these challenges, Renewable Energy Sources (RES), and Energy Storage Systems (ESS) can be integrated into the design of UFCS. If well-planned, the incorporation of wind turbines, PV panels, and ESS in the UFCS not only increases the sustainability of the station but can also allow lifecycle economic savings for the entire structure. Nevertheless, to take advantage of the benefits coming from the integrated charging station, the design must be well-managed. In fact, on one side, an oversize of RES and ESS capacities will lead to a waste of resources and money, on the other side, instead, an undersized capacity which does not meet the charging demand will not avoid the large purchase of electricity from the national electric grid.

In literature the integration process of renewable sources and energy storage system within EVs charging stations has already been faced with various approaches. In the following, a survey of the existing research conducted on BESS and RES integrated UFCSs is presented. Within this review, a literature gap can be recognized that justifies the objectives of this work. A huge part of the existing studies related to the mitigation of the impact of EV charging on the public electric grid analyze coordinated charging techniques[7]–[9] and incorporate RES with ESS for slow charging applications [10], [11]. However, most of these works cannot be directly applied to extreme fast charging (XFC) applications because of the power demand profile changes and the differences in charging objectives the two technologies (Ultra-fast and slow) have.Few papers investigate the integration of renewables and/or energy storage in EV fast charging applications [12]–[15]. In [12] the authors propose a mixed integer linear programing (MILP) formulation for determining size and type of RES and ESS to be installed in a fast charging station, their aim is to minimize the energy cost associated with the charging infrastructure. In [14] instead a bi-objective optimization algorithm is presented which aims to minimize the Cost Of Energy (COE) of the FCS as well as its environmental impact. The bi-objective function is resolved by a mix algorithm, which combines multi-objective particle swarm optimization (MOPSO) algorithm and Technique for Order Preference by Similarity to Ideal Solution (TOPSIS) method. A Genetic Algorithm (GA) single-objective optimization problem whose goal is to maximize the Net Present Value (NPV) of the charging station by integrating RES and BESS is depicted in [15]. However, none of these studies consider the number of cycles and cycle depth of the battery and hence any battery degradation model. Moreover, even if the optimization is applied to fast charging stations in these papers, the maximum charging rate of a single charger never exceeds the value of 50kW.

In most of the literature associated to charging stations optimization, the demand profiles used are very simple. For instance in [16] the authors use a constant power demand in their optimization for sizing the PV system to be inserted in the charging station design. In [17] and [18] the authors do not consider any battery characteristics of any vehicle and just set the output power of each charger to a fix value. In [19] only one EV typology has been taken in the study. In [20] and [21] instead the authors considered different electric cars typologies with different battery capacities however all characterized by a constant charging profile. More complex models take into account usually different queueing theories. For instance in [22] and [23] a model based on an M/M/s queueing theory is used. However, in all these studies, no one considers different EVs typologies or models and takes into account the differences existing in the charging profiles as well as the dependence of the charging rate from the SOC.

The main goal of this work is to define an optimal solution that allows a successful integration of a PV power plant and a BESS within an Ultra-Fast charging station. Initially, the study focuses on the UFCS load forecast for an entire year using a minute-by-minute algorithm. Then, the optimization algorithm necessary to perform the integration of the PV plant and BESS is explained along with all the models used to simulate the system components. The final aim is a technical-economical optimization of the final configuration which comprises a PV system, a battery storage, a connection to the grid and the Ultra-Fast chargers which compose the station. The final configuration is gradually reached; indeed, the first step is coupling the PV plant and optimizing its size by maximizing the Net Present Value (NPV). Then, the configuration completed with the storage system is analyzed and the size of the BESS is found too. Lastly, a sensitivity analysis concerning the PV and BESS sizing is performed. This last analysis aims to study the dependency of the results on various kinds of parameters, trying to exploit different scenarios varying their values and analyzing the related results.

The originality of this paper is as follows:

- In the load demand computation, the power supplied by each port is limited by the vehicle charging capability and not by the infrastructure, since the study focuses on UFCS.
- The power demand estimation considers different types of EVs such as cars, motorbikes, and heavy-duty vehicles.
- Intermediate configurations have been analyzed in order to prove the convenience of the final one composed of PV modules, BESS, and the national electric grid.
- Different Energy Management Strategies (EMS) are discussed in the sensitivity analysis.

The paper's structure is defined in the following. The system model and its each component are described in Section II. The proposed optimization process is presented in Section III. Section IV examines the results and the performances of the various configurations. In Section V a sensitivity analysis is presented, and, finally, Section VI concludes the paper.

II. System Model

In this section the system layout and the models of each component are presented. The proposed configuration for the charging station is reported in Figure 2. All the components are connected to a DC bus, directly linked with the charging points. The energy flow can be bidirectional only in correspondence of the battery and of the connection with the grid. This configuration has been selected in order to minimize the number of AC/DC conversion and to better integrate all the DC components. With fewer conversion stages an improvement of both the efficiency and the cost of the overall system is possible. For instance, in [24] authors estimate that in DC bus systems the conversion losses can be decreased from about 32% to less than 10% with respect to an AC bus architecture. With a DC bus architecture is also easier to integrate Renewable Energy Sources (RESs) and Energy Storage Systems (ESSs) that can be used to mitigate the negative impact of the UFCS on the distribution MV grid [25]. This fact must not be underestimated, as a matter of fact in [26] authors shown that fast charging stations can increase the peak demand by about 9%. The Vehicle-To-Grid technology, which foresees a bidirectional flow of energy between the EVs and the DC bus, is not contemplated in this application. Indeed, Ultra-Fast Charging aims to recharge the batteries as fast as possible and therefore in this situation the EV users are not expected to be interested in V2G technology.

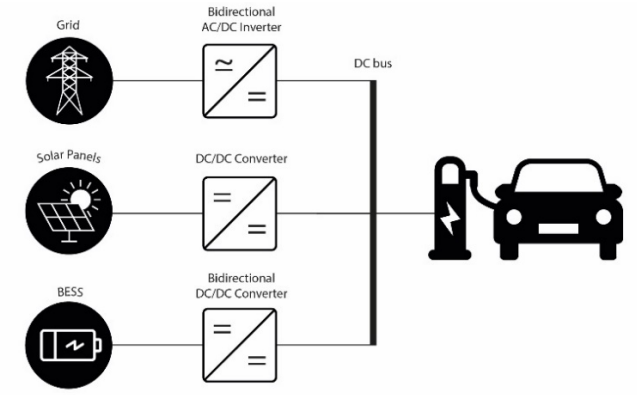

Figure 2 Charging station configuration

Since this charging station is targeted at a highway application, the most suitable solution is to implement Ultra-Fast charging process which differs from standard charging stations thanks to higher charging power (from 150 kW up to 300 kW for every charger) that ensures a full of energy in charging times about 25-35 minutes.

A. Charging Load Demand

The load curve is the trend of the charging station demanded power throughout a time period, in this case 24 hours. The charging power demand trend for an entire typical year is obtained by the arrangement of three days macro categories: weekday, weekend and August weekday. A considerable number of input data are needed to plot such a profile, and because of the unavailability of historical data regarding this new load for the electric grid, a probabilistic approach has been followed. The vehicle density probability distributions for the three different scenarios (weekday, weekend, and August weekdays) are reported in Figure 3. These functions have been achieved by considering the actual traffic flow data provided by the Italian National Road Authority [27]. These data refer to a service area with a gasoline station installed along a highway in Italy.

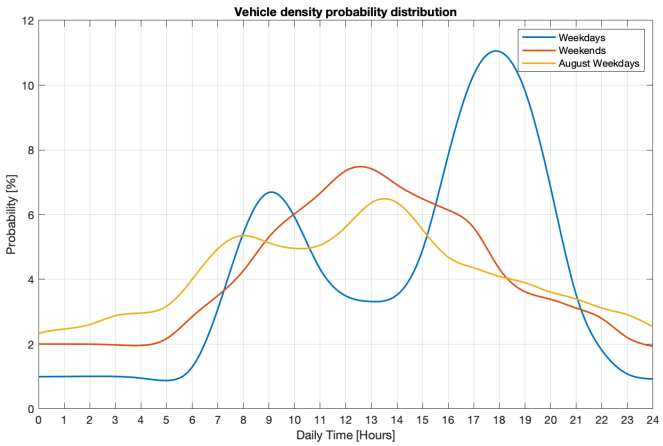

Figure 3 Vehicle arrival distribution.

Once defined the arrival probability distributions, the vehicles categories are specified. In this study, to take into accounts all the different charging behaviors of the existing electric vehicles six categories are considered: three car sizes (Large, Medium and Small) which differ for the capacity of the battery and all the features that come with that, two heavy vehicles (trucks and buses) and electric motorbikes. The percentages of each category on the whole number of vehicles are carefully selected according to the day and the electric vehicle market share in Italy [28], as shown in TABLE 1.

TABLE 1
VEHICLE FLEET SHARE PERCENTAGE.

	Cars (35% EV)	**Heavy vehicles** (30% EV buses, no EV trucks)	**Bikes** (10% EV)
Weekdays	**60%** *40% L, 40% M, 20% S*	**35%** *10% buses, 90% trucks*	**5%**
Weekends	**90%** *40% L, 40% M, 20% S*	**5%** *100% buses*	**5%**
August Weekdays	**70%** *40% L, 40% M, 20% S*	**25%** *20% buses, 80% trucks*	**5%**

The next step is to precisely define the charging profiles that each vehicle follows to complete its charging process. Indeed, the actual charging power does not depend only on the size of the charger, but it is defined also by the vehicle charging capability, which in turn depends on multiple factors such as the battery capacity and the external temperature. To simulate this feature, the charging profiles of three different electric car commercial models have been taken as reference:

- Large: Audi e-tron GT, battery 95 kWh.
- Medium: Volkswagen ID 3, battery 58 kWh.
- Small: Nissan Leaf, battery 40 kWh.

As regards the bike category a model with a battery capacity equal to 21.5 kWh is selected. Lastly, to represent the charging behavior of the heavy duty vehicles, a general truck/bus with battery capacity of 250 kWh and a constant charging power of 200 kW is considered. The charging profiles of all the considered EVs are reported in Figure 4 [25].

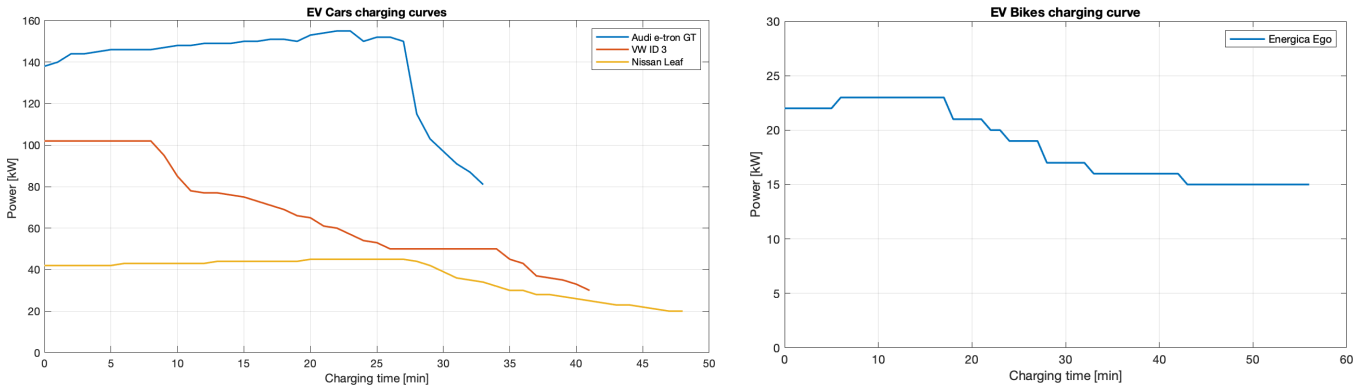

a) b)

Figure 4 EVs charging profiles of a) electric cars and b) electric motorbike.

To estimate the State of Charge (SOC) of the arriving EVs a Weibull distribution has been used, and its trend is reported in Figure 5 [29]. As can be seen, EVs performing long-distance travels are expected to charge their vehicle at SOC in the range 10–30%, with a peak probability at 20% [30].

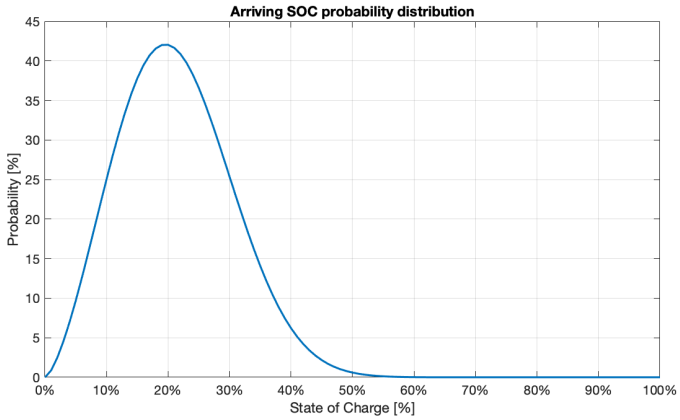

Figure 5 Arrival SOC probability distribution.

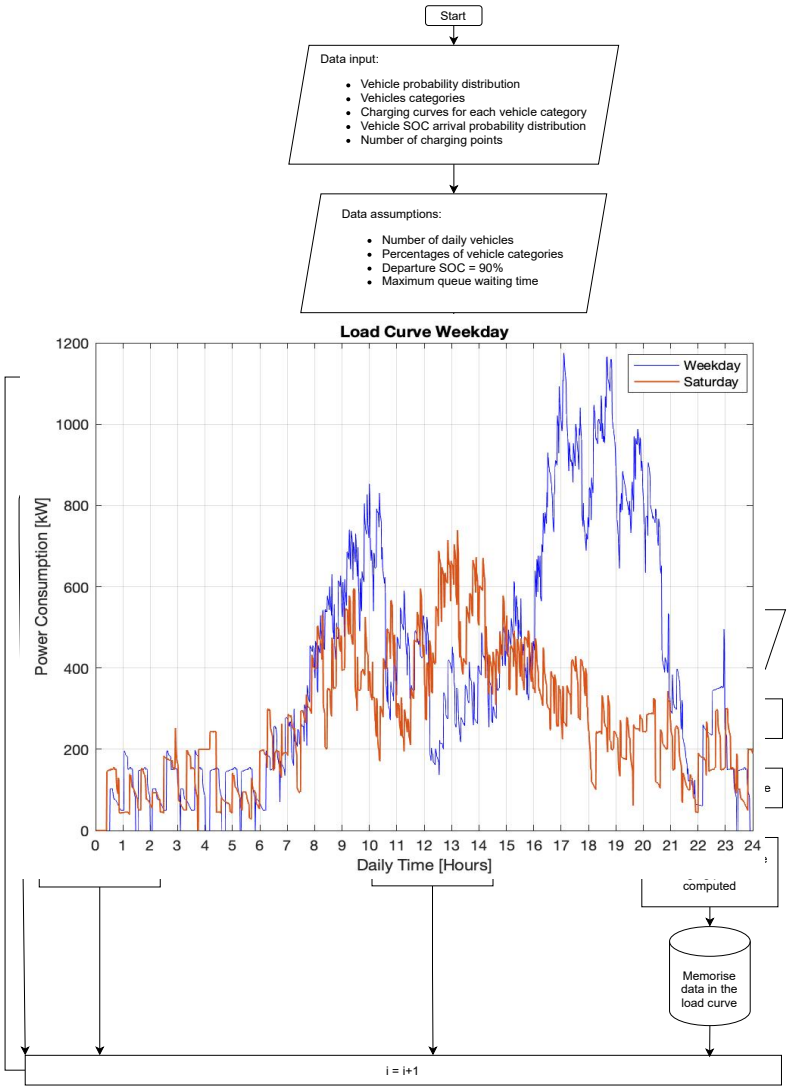

Figure 6 Power demand flowchart.

In this study the UFCS is assumed having 10 charging points with a maximum charging power of 200 kW and 15 minutes of maximum waiting queue time allowed. By following the steps described in the flowchart depicted in Figure 6, the following results have been obtained. In Figure 7 the charging station load curve obtained for a weekday and a weekend day is reported. The weekday curve is characterized by two different peaks of power during the day: a smaller one in the morning and the highest during late afternoon. On the other hand, during weekends, the curve is more linear, and it reaches the maximum power required at midday. The other difference is the amount of power required, during weekdays the load curve reaches almost 1.2 MW. This gap is mainly given by the affluence difference between the two days. In Figure 8 the number of occupied charging ports inside the station throughout the day is portrayed. As shown in the graph, the station has 10 charging points simultaneously usable. It represents a trade-off solution in order to guarantee a high utilization rate for every CP and to avoid too long vehicle queues. Using this procedure, the daily curves for an entire year are computed. Specifically, it is worth highlighting that using this simulation algorithm, even days of the same categories show significant differences in their load curves. This feature allows to reflect reality as much as possible and gives credit to the simulation, reducing the need of carrying out a sensitivity analysis on the load curve parameters. Furthermore it has been chosen a time frame of one year for several reason: smoothing the randomicity effect of the code, use all the typical days considered, have a time period suitable for the exploitation of different scenarios for the photovoltaic power production. The resulting amount of energy yearly required by the charging station is equal to 3,251.5 MWh.

Figure 7 Power load curves.

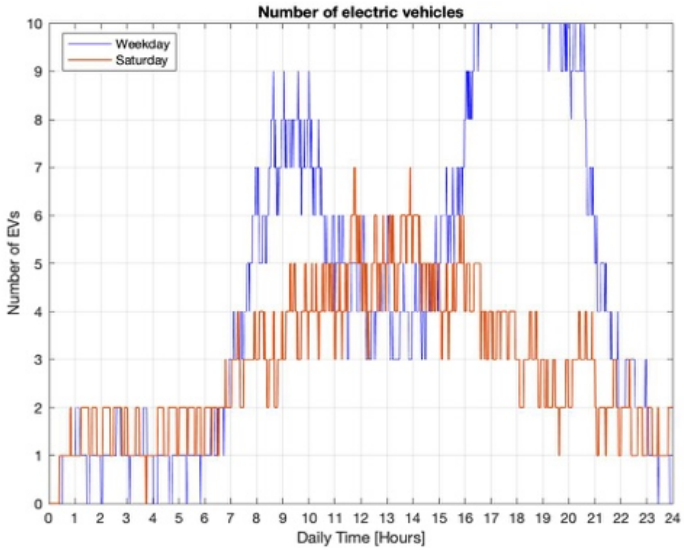

Figure 8 Occupancy of charging ports.

B. Photovoltaic System Model

Usually, in literature, the photovoltaic power production is forecasted starting from the irradiance values and the temperature, with the following formula:

$$P_{PV}(t) = f_{PV} \cdot \left(\frac{i_t(t)}{i_s}\right) \cdot \left[1 + \alpha_p \cdot (T_c - T_s)\right] \quad (1)$$

where f_{PV} is the derating factor, $i_t(t)$ is the global solar radiation incident on the PV module [kW/m^2], i_s is the incident standard radiation, equal to 1000 W/m^2, α_p is the temperature coefficient and for a polycrystalline silicon module is equal to -0,48%/°C, T_c is the cell temperature of PV modules and T_s is the temperature of PV panel at standard condition (25°C).In this case the PV production is computed in power unit, a suitable approach for this study since the PV power installed will be an output of the optimization process. With this method, a typical day of solar production is considered for every month. In Figure 11 the typical PV production in power unit is reported for every month. However, considering the same PV production for every day of the month, without any spikes or holes due to shading, is an easy solution but not a realistic one. Therefore, in this paper, a different approach is exploited to obtain a more reasonable PV power production, which varies every day of the year. To estimate the PV profile, the PV performance tool of PVGIS has been used. Indeed, this tool has allowed getting the power produced in the specific charging station location every day for several years. Then, a day-by-day average of the data of all the years has been done in order to obtain a typical year trend. As an example, in Figure 10 the PV production in power unit is reported for 5 days of two months characterized by different solar irradiation.

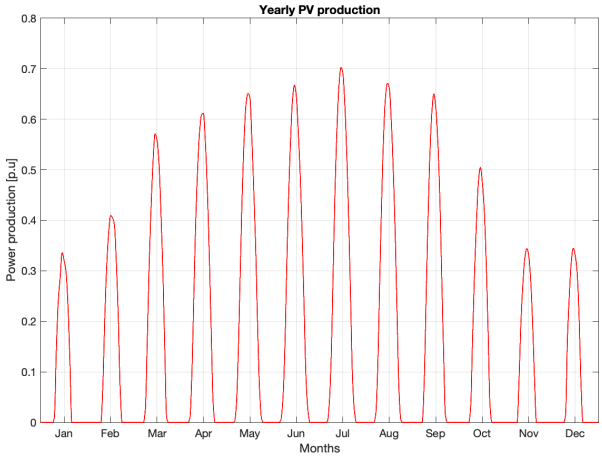

Figure 9 Estimated average PV irradiance for every month of the year.

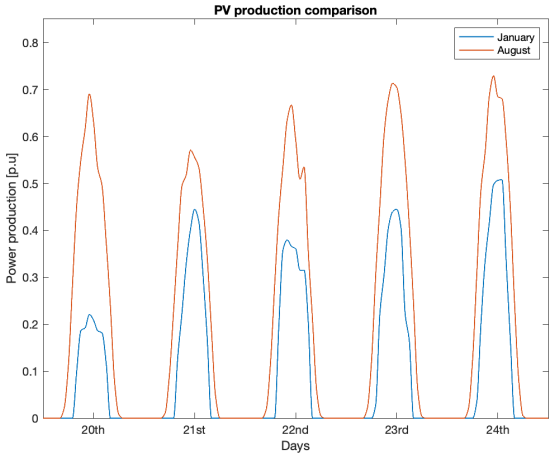

Figure 10 PV irradiance in 5 different days.

C. Energy Storage System Model

For this application, a Li-ion BESS is considered since this technology ensures the best performances [31]. Indeed, this kind of BESS is also capable of rapidly changing the working conditions to cope with the fast load and PV production variations. Clearly, to create a realistic model of the whole station, some constraints related to the BESS shall be addressed: firstly, the charging efficiency η_{BESS}^{ch} and the discharging efficiency η_{BESS}^{dis} are introduced, respectively equal to 96% and 92%. Furthermore, the lifetime of the battery pack is limited to a certain number of cycles, 3000 in this case. Once reached this value, the replacement of the battery pack occurs. The number of cycles is computed with the following formula:

$$N_{cycles} = \sum_{d=1}^{365} \sum_{t=1}^{1440} \frac{|SOC_t - SOC_{t-1}|}{2 \times DoD} \tag{2}$$

where DoD is the Depth of Discharge, SOC_t and SOC_{t-1} is the state of charge of the battery at time *t* and *t-1*, respectively. This parameter is equal to 0.8 since the BESS can be used with an SOC ranging from 10% to 90% in order to preserve its duration. Lastly, the C-rate is another parameter to consider while characterizing a battery energy storage system. Specifically, the C-rate is the ratio between the nominal power of the battery [W] and its capacity [Wh]. The standard configuration includes a BESS with a C-rate of 1/2: as a consequence, the battery is completely discharged in 2 hours.

III. Optimization Problem

All the inputs presented in the previous sections are used to build up the station mathematical model. The optimization process aims to define the components size in order to maximize the economic benefits. Two different scenarios are analyzed. In the first one only the PV system is integrated in the station design; in the second and complete one instead both the PV system and the BESS are simultaneously introduced and sized.

A. Objective function

Since the aim of this work is to maximize the profitability of the whole system, economical parameters will largely affect the sizing process. Starting from the energy prices, three different values are considered:

- Selling price of energy at the EV costumers, equal to 70 c€/kWh.
- Purchase price of energy from the grid, equal to 17.46 c€/kWh.
- Selling price of energy to the grid, considered equal to 1/10 of the purchased one.

The economic criteria used to analyze the profitability of a certain configuration is the Net Present Value and its formula is reported in (3):

$$NPV = -CAPEX_k \cdot P_k - Repl_k \cdot E_k + \sum_{year=1}^{lifetime} \frac{CashIn_{yearly} - CashOut_{yearly} - OPEX_k \cdot P_k}{(1+r)^{year}} \tag{3}$$

where P_k is the power of the *k-th* component (PV and BESS), E_k is the energy of the *k-th* component, $Repl_k$ is its replacement cost, $CashIn_{yearly}$ is the yearly income earned selling energy to EV owners and $CashOut_{yearly}$ the yearly expenses due to the purchase of energy and r is the discount rate. The numerical values used for these parameters are reported in TABLE 2.

TABLE 2

NUMERICAL VALUES.

Parameter	Value
$CAPEX_{PV}$	1,000 €/kW
$OPEX_{PV}$	160 €/kW/year
r	2.5%
$CAPEX_{BESS}$[a)]	439 €/kWh
$Repl_{BESS}$	196 €/kWh
$lifetime$	20
$OPEX_{BESS}$	4.28 €/kWh/year

a) Considering discharging rate of 0.5 (2 hours).

B. Constraints

The maximum value of NPV must be found by assuring that the following constraints are always satisfied:

1) power balance: the system must meet the power balance, which means that the power required by the connected vehicles (P_{EV}) has to be equal to the sum of the power provided by the PV panels (P_{PV}), the BESS (P_{BESS}^{ch} and P_{BESS}^{dis}), and the grid (P_{gr}) in every instant of time *t*. This balance is described in (4), where η_{ch} is the efficiency of the EV charger, η_{BESS}^{ch} and η_{BESS}^{dis} are the charging and discharging efficiency of the BESS respectively, $\beta_1(t)$ and $\beta_2(t)$ are binary variables which define the operation of the battery.

$$\frac{P_{EV}(t)}{\eta_{ch}} - P_{PV}(t) + P_{BESS}^{ch}(t) \cdot \eta_{BESS}^{ch} \cdot \beta_1(t) - \frac{P_{BESS}^{dis}(t)}{\eta_{BESS}^{dis}} \cdot \beta_2(t) = P_{gr}(t) \tag{4}$$

2) Battery charge/discharge: a constraint which forces the battery to cannot be simultaneously charged and discharged is needed and it is expressed in (5).

$$\beta_1(t) + \beta_2(t) = 1 \tag{5}$$

3) BESS design: these constraints include the limits related to the BESS component reported in (6) and (7). The limit in (6) express the fact that the charging and discharging power ($P_{BESS}^{ch,dis}$) of the BESS cannot exceed the maximum value declared by the manufacturer (P_{BESS}^{max}). Finally, the restriction in (7) highlights that the energy of the battery (E_{BESS}), in every instant of time *t*, cannot surpass the minimum (E_{BESS}^{min}) and maximum (E_{BESS}^{max}) limits.

$$P_{BESS}^{ch,dis}(t) \leq P_{BESS}^{max} \tag{6}$$

$$E_{BESS}^{min} \leq E_{BESS}(t) \leq E_{BESS}^{max} \tag{7}$$

C. Photovoltaic integration algorithm

Basically, the aim of the MATLAB algorithm is to compare the power demand of the station with the PV production in order to drive the energy management to a sustainable behavior of the station. In Figure 11 a flowchart describing the algorithm followed to compute the NPV of this scenario is reported. For clarity purposes a color scheme is adopted: green characterizes the condition in which the station is independent from the grid, red instead, is used for the case in which grid power is needed.

The algorithm is outlined by two concatenated *for* cycles: one that runs through each day of the year and one that runs through each minute of the day. In every minute, the comparation between the power produced by the PV power plant and the power demanded by the charging station is performed; from this point two different possibilities arise. Even graphically, these two possible conditions are differentiated in colors: if the power demand is higher than the PV production, all the solar energy is used to supply the load and the remaining demanded energy is bought from the grid. Doing so, the self-consumption of the station is equal to the totality of the PV power produced. This condition is colored in red, and it is characterized by grid intervention to cover the power demand. On the other hand, if the PV power produced exceeds the power demand, the entire load is covered by the renewable energy, and the self-consumption of the station is equal to the power demand. This condition is colored in green: with respect to the previous case, here the station is independent from the grid, and the station impact decreases.

Finally, at the end of each day the amount of energy sold to EVs is saved, and the cash flow is computed: the cash-out is equal to the energy bought from the grid multiplied for the buying price, and the cash-in is the energy sold to EVs times the selling price. The process is performed for each simulated day of the year.

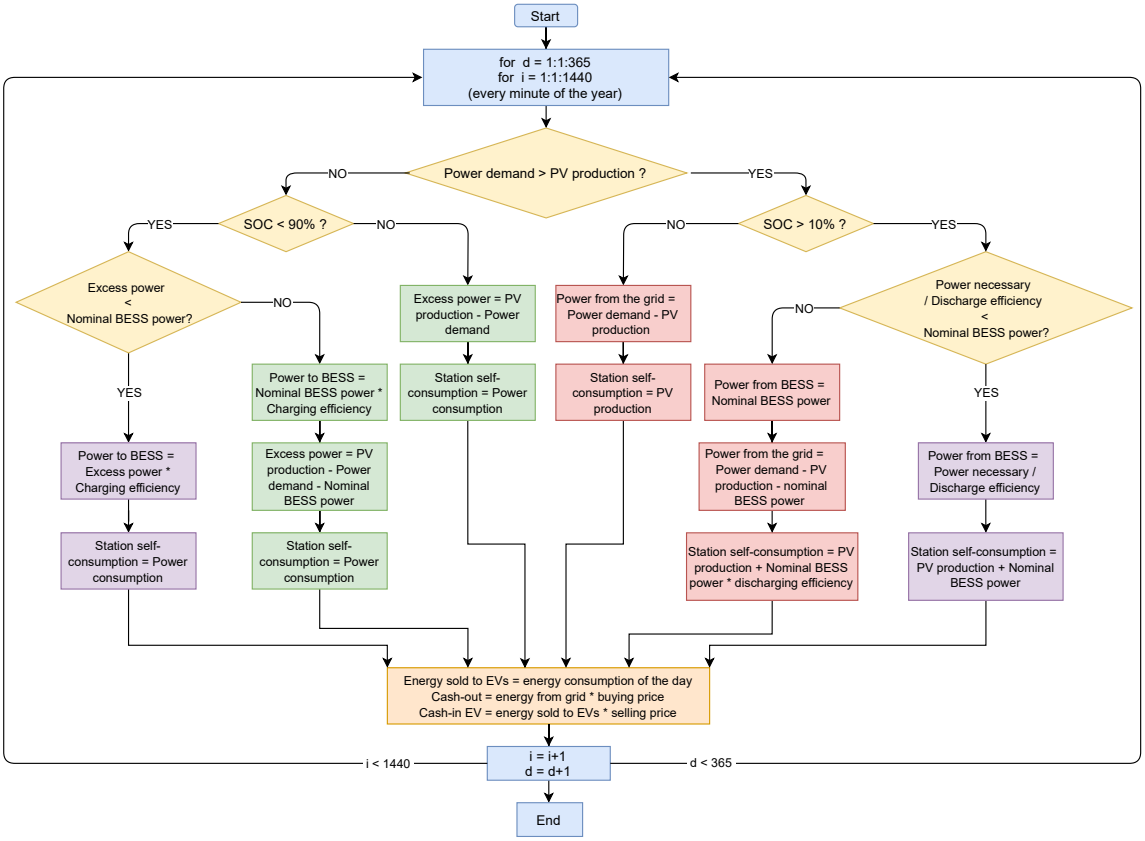

Figure 11 PV+BESS integration algorithm flowchart

D. Photovoltaic and battery integration algorithm

Following the same procedure of the PV coupling, the algorithm that drives the BESS coupling with the system is presented in this paragraph.

In Figure 11 a flowchart describing the algorithm is reported. Even in this case a color scheme is adopted: with this configuration another color is added to red and green ones. Purple defines the conditions in which the PV plant is not able to cover the power demand, but grid power is not needed thanks to the BESS implementation. Two *for* cycles are exploited even in this case to analyze each minute of each day through a year: in each minute, to define the behavior of the various components, three conditions are evaluated. The first one compares the power demand and the PV production; the second one defines if the BESS can be exploited relying on its SOC, and the third one makes sure that the power exchanged with the BESS is within its power limit. From these conditions, six different types of behavior can be derived. Hereafter, a summary of these behaviors is presented.

Starting from the first condition, if the power demand is higher than the PV production, the BESS should provide the remaining demanded power whenever is possible. Clearly, if the BESS SOC is below the minimum threshold of 10%, the BESS cannot be used (red condition). If the remaining power required by the load is greater than the BESS power limit, it provides its nominal power and the additional power to close the gap with the load is bought from the grid (red condition). If the BESS is capable of covering the totality of the power demand, the station keeps on being independent from the grid (purple condition). On the other hand, if the PV production is greater than the power demand, the excess power should be stored in the BESS whenever is possible. If the BESS can get the entire excess power, the latter is stored (purple condition). If the battery SOC is over its maximum threshold of 90%, energy cannot be stored anymore but the station maintains its stand-alone capability (green condition). Furthermore, if the excess power overcomes the BESS power limit, the battery will be charged only at its nominal power. Nevertheless, the station still works stand-alone (green condition). At the conclusion of the *for* cycles, the same computations of the previous case are carried out: the energy sold to EVs, and the cash flows are calculated in order to perform the final optimization.

IV. Results and Discussion

The target of these optimizations is to maximize the NPV, varying the size of the station components: the PV peak power and the BESS capacity. The tool selected to carry out the simulations is MATLAB and in particular its add-on called *global optimization toolbox*. The economical benchmark introduced is the NPV of the charging station without the PV plant and the BESS, which is characterized by the purchase of all the energy needed from the grid. This NPV is equal to 26.6 M€.

A. PV power plant coupling

The first configuration analyzed includes the station coupled only with the photovoltaic power plant. The basic array used for the optimization is composed by 40 *Conergy PowerPlus* panels (250Wp) installed in series, reaching a maximum power of 10 kWp. The final size of the PV power plant is obtained as a multiple of this value.

The optimal dimension of the photovoltaic system is 1.24 MW, which leads to an NPV equal to 28.74 M€. The income increases by almost two million of euro compared with the "only grid" case. During a whole year, the energy bought from the grid drops from 3.25 GWh to 1.91 GWh thanks to the installation of the PV power plant. This configuration also brings a high value of energy surplus (557 MWh); this surplus occurs when the PV production is higher than the load curve, and it is more evident during summer months as shown in Figure 12.

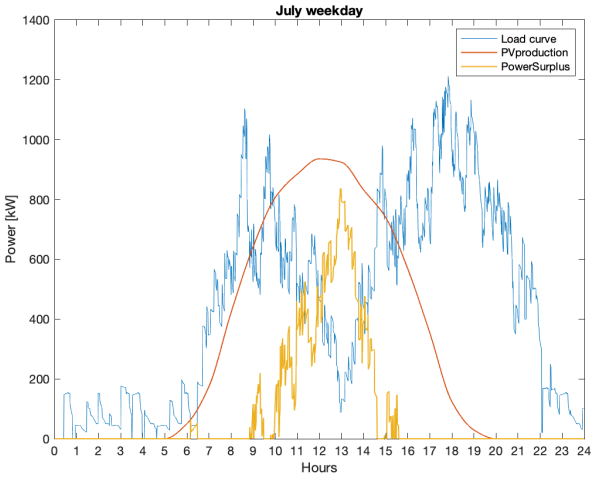

Figure 12 Daily power trends in day 200.

During the hottest hours of the day, the power surplus reaches a peak of 800 MW, bringing the necessity to couple an energy storage system. Obviously, the situation is different for winter months but not only. In Figure 13, PV production and load curve are reported for an October Sunday.

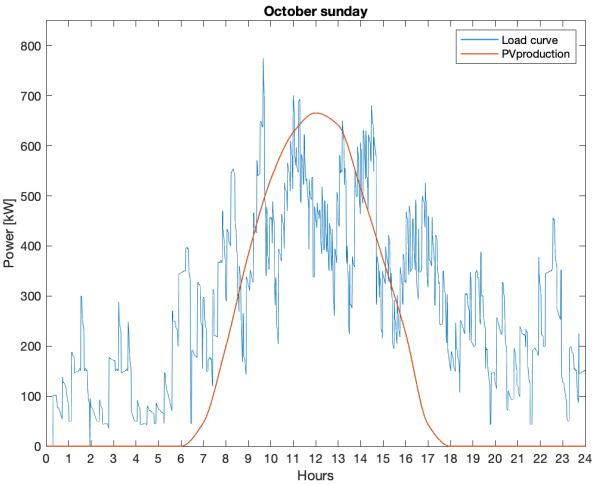

Figure 13 Load and PV power in day 287.

The typical weekend load curve is more suitable for the integration of a PV power plant since the peaks of the two curves are quite coincident. The daily power surplus during august reaches very high values due to two different reasons: the high solar irradiance in a summer month and the lower power required by the charging station. In Figure 14 this trend could be appreciated by the high amount of energy surplus during the day.

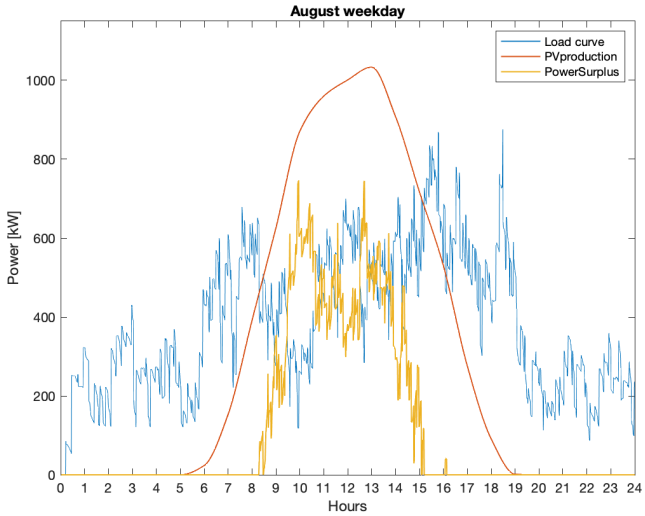

Figure 14 Daily power trends in day 229.

The energy surplus during this day is equal to 2.75 MWh, 32% greater respect to the energy surplus during the July weekday reported before.

B. PV and BESS coupling

The integration of an energy storage system could be a suitable solution to avoid wasting energy and decrease the dependency of the charging station from the grid. In this case the NPV is maximized varying together the size of the PV power plant and the BESS. Even for the energy storage system a base battery pack is considered to drive the sizing process: a 10-kWh module is selected.

The NPV obtained is higher with respect to the only PV case and is equal to 28.78 M€. The photovoltaic plant is slightly bigger than the previous case and is equal to 1.30 MW. Thanks to the implementation of a battery with a capacity of 770 kWh, the increased solar energy produced can be stored and sold to the EV costumers.

In this case, the energy bought from the grid is significantly lower thanks to the better exploitation of the PV energy; its yearly value is 1.69 GWh on a total of 3.25 GWh required by the charging station, almost 50%.

An example of the BESS behavior is reported in Figure 15, where the SOC trend is reported together with the PV production and the load curve. In this case an August weekday is analyzed.

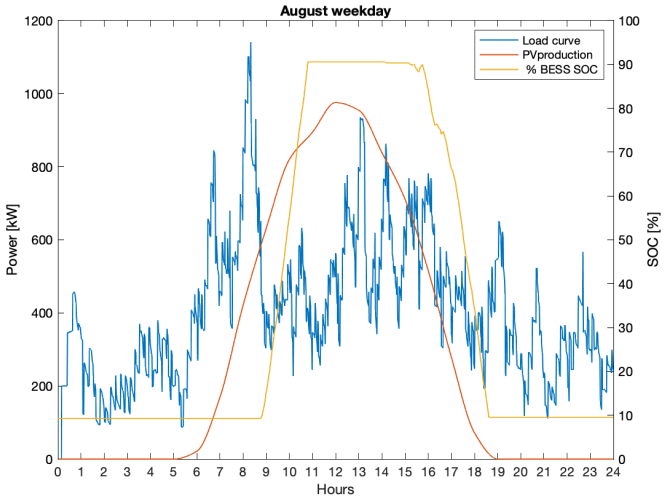

Figure 15 Daily trends in day 237.

The BESS is completely charged during the morning; the stored energy will be exploited in the late afternoon, when the load curve overcomes the PV production. Looking solely at this graph, the BESS size can be intended undersized due to the fast achieving of the maximum SOC. However, considering a trade-off between all the days of the year and the BESS installation costs, this is the optimal from an economic point of view. To better evaluate the variety of behaviors, the comparison between power surpluses during three different months is reported.

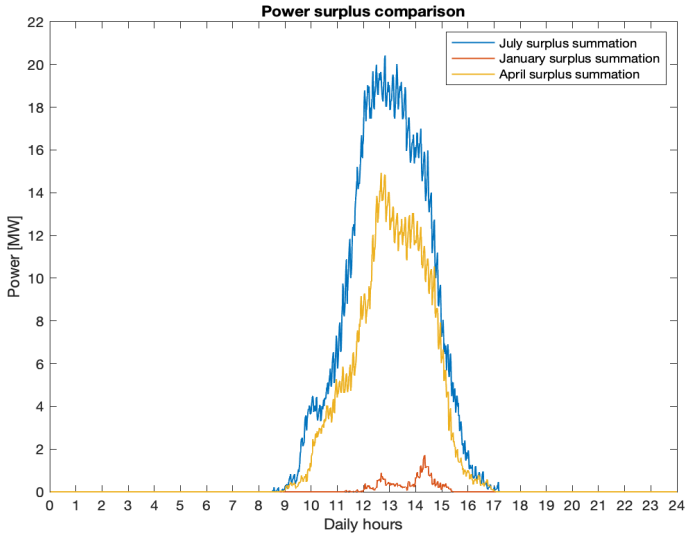

Figure 16 Power surplus in January, April and July.

The comparison between summer and winter is remarkable, and it underlines how different the behavior of the entire station system is between two different year period.

C. Results comparison

In this paragraph a results comparison will be developed trying to understand how the investment costs for the BESS and for a greater PV plant are recovered. The installation of a greater PV system increases the yearly solar energy produced by 102 MWh. The yearly energy bought from the grid decreases by 219 MWh, approximately 11% of the total energy purchased, resulting in a yearly saving of 38 k€. The energy surplus decreases by 142 MWh: approximately 25% of the energy wasted in the only PV scenario.

The difference is evident also during the daily analysis of the power trend. For example, in Figure 17 the energy bought in the two configurations are compared for a June weekday.

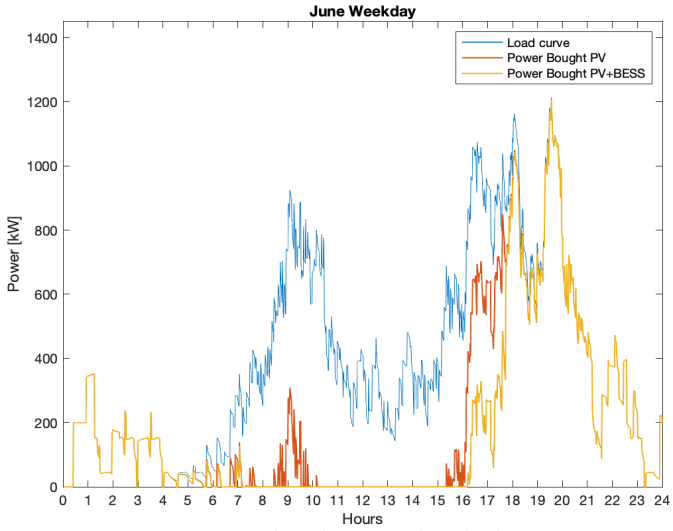

Figure 17 Energy bought comparison in day 169.

The stored energy is used not only during the afternoon, when the load curve overcomes the PV production, but also during the central hours of the day. Indeed, the red curve shows a peak of energy bought around 9 a.m. that is avoided thanks to the BESS coupling. Together with the reduction of the energy bought from the grid, the implementation of a BESS will reduce the energy surplus wasted or sold to the grid. The difference between the only PV scenario is shown in Figure 18 for a March weekday.

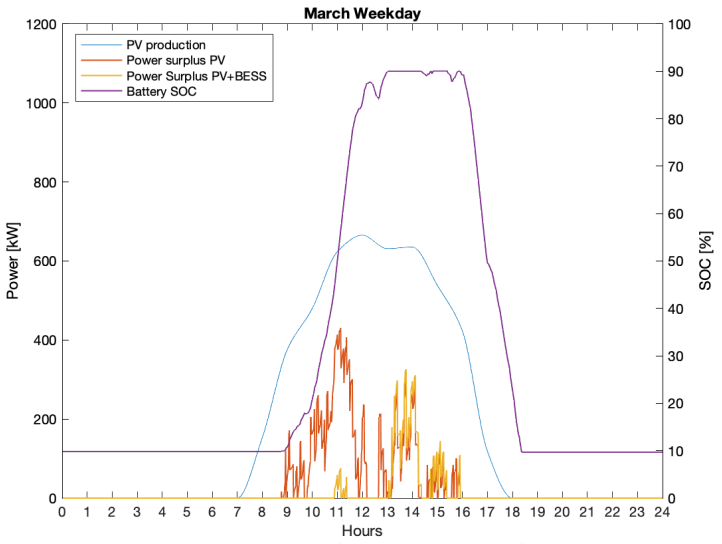

Figure 18 Power surplus comparison in day 63.

Comparing the red and the yellow line, it is clear how the possibility to store the energy is perfectly combined with this type of system. The daily energy wasted decrease by 0.54 MWh with respect to the only PV case (0.83 MWh), almost 65% of its original value.

V. Sensitivity Analysis

Starting from the results obtained in the previous scenarios, their evolutions are analyzed varying significant parameters, to better comprehend their dependency and to foresee future scenarios.

A. Capex Variation

Throughout the computations, a stringent limit in the components sizing was put in place by CAPEX and OPEX parameters. The values considered in the previous chapter are expected to drop in the next years and a forecast is reported in Figure 19. These expenditures drops are expected not only because the concerning core technologies are under heavy development in recent years, but also because in the near future, materials and production processes will be standardized and more accessible. Furthermore, these applications will be more and more diffused, ensuring levelized initial investments [32].

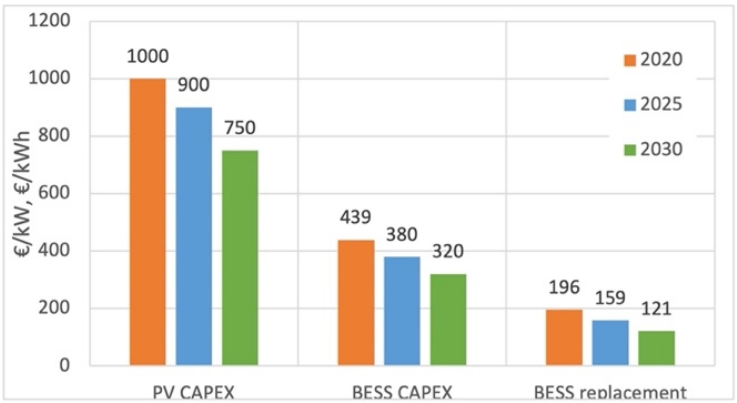

Figure 19 CAPEX and replacement cost forecast.

Clearly, with this lower investment costs, the sizing of the PV plant and of the storage system will be more extensive, resulting in a more sustainable UFCS. In TABLE 3 an overview of the obtained results is reported.

TABLE 3
CAPEX Sensitivity Analysis Results.

Year	**Station configuration**	**NPV** [€]	**PV peak power** [MW]	**BESS capacity** [MWh]

2025	PV	28 867 253	1.30	/
	PV+BESS	29 008 693	1.48	1.1
2030	PV	29 070 710	1.41	/
	PV+BESS	29 447 554	1.77	1.99

The interesting fact tough, is that not only the NPV is greater throughout the years, but the size of the PV plant and BESS increase consistently. For the 2030 scenario, the PV field and the BESS capacity are respectively 31.5% and 158% bigger with respect to 2020. These results are encouraging not only from the economic standpoint, but also from an environmental one: in the future this UFCS could have a renewable self-production of 62%. With this feature, the station will be able to deliver more than half of its from green sources and this trend will help reducing the environmental impact of the transportation sector.

B. Energy Sold to the Grid

In all the configurations and cases considered until now, the sale of surplus energy to the grid has never been considered. The energy considered for the sale is just the surplus component that occurs when the PV power plant is producing enough energy to overcome the load and the possible BESS charging thresholds. It requires the installation of a system able to reverse the power flow when needed. The NPV increases by 130 k€ respect to the base case, this difference has to justify the investment for such bidirectional components. Even the optimized size components are different, leading the PV power equal to 1.46 MW and the BESS capacity equal to 1,032 kWh, respectively 12% and 34% bigger respect to the base case. The yearly self-consumption energy increase by 3.7% respect to the base case and it brings a saving of 21.4 k€ every year. This value can be compared with the revenues given by the purchase of energy to the grid. The energy sold bring a yearly cash-in equal to 9,1 k€. So, the increased profitability comes mainly by the savings for the less energy bought that from the revenues of the energy sold.

C. Battery Discharging Rate

In this section, the battery duration parameter will be varied to establish how the optimal solution of the optimization problem is influenced. Three different possibilities are exploited for the duration of the battery: 1 hour, 4 hours and 6 hours, which correspond to 1C, 0.25C and 0.167C charge rates (C-rate) respectively. It must be highlighted that for the same nominal energy capacity, the cost of a battery with lower power performance in terms of C-rate is cheaper; the differences is valid not only for the battery pack, but also for the others electronic devices like the inverter. In Figure 20 the prices for all the analyzed configuration are reported.

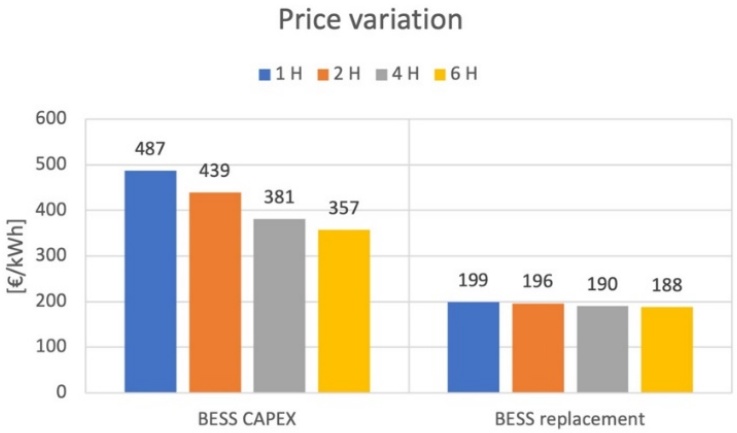

Figure 20 Prices for different BESS duration

In TABLE 4 the optimization results for the different C-rate of the battery are reported.

TABLE 4
BESS DURATION SENSITIVITY ANALYSIS RESULTS.

BESS duration	NPV [€]	PV peak power [MW]	BESS capacity [kWh]	BESS power [kW]
1 h	28 737 474	1.23	670	670
4 h	28 832 070	1.39	900	225
6 h	28 831 946	1.39	1,100	183

The best results are obtained for the case with a battery duration of 4 hours. Indeed, in this case, the lower CAPEX allows an installation of a battery with a 17% higher capacity with respect to the base case, and the consequence is a growth in the PV size. The strong reduction of the BESS nominal power, 42% smaller respect to the base case, will not cause a worsening of energetic and economic performances. The resulting NPV starts to decrease with the 6 hours battery duration. Indeed, for this case, all the reasonings related to an increased BESS capacity due to a CAPEX reduction are still valid. However, the NPV is slightly lower with respect to the previous case and the low BESS power is the reason. This drawback is perfectly shown in Figure 21.

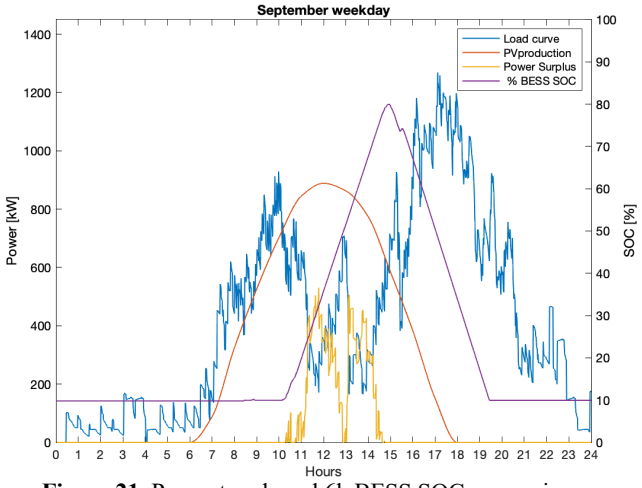

Figure 21 Power trends and 6h BESS SOC comparison

During the mid-hours of the day, the PV production overcomes the load curve and the BESS, due its limited power, is able to store the solar energy only partially. It brings a high-power surplus and a partial exploitation of the battery capacity since its SOC does not reach the maximum value but it stops at 80%. In conclusion, from the results it is clear how, for this kind of applications, the capacity of the storage system is more important than its power performances till a certain threshold that is highlighted in this sensitivity analysis.

D. Grid energy purchase price variations

In this section two different concepts are introduced: the first one is purely economic and, as already mentioned, is the energy price differentiation following time bands. This segmentation already exists in the Italian electricity market, and it is shown in TABLE 5. The second concept introduced in this paragraph is a direct result of the first one and it is related to the energy management of the BESS. Due to the price difference of energy between daily hours and the night, the possibility to charge the BESS during F3 is introduced, in order to use the stored energy for the self-consumption during F1 and F2, when the energy price is higher.

TABLE 5
ITALIAN ELECTRICITY MARKET TIME BANDS.

	F1	F2	F3
Monday-Friday	8 am–7 pm	7 am– 8 pm. 7 am– 11 pm.	00 – 7 am 11 pm – 00
Saturday	/	7 a.m. – 23 p.m.	00 – 7 am 11 pm – 00

Sunday	/	/	All day

To introduce differences between time bands energy prices, a brief study on the possible price deltas has been carried out. In particular, the percentage difference has been incremented from 10%, running simulations with the aim of identifying the best conditions for the charging station. In addition, the situation of the Italian electricity market has been monitored in order to find not only a suitable solution from technical standpoint, but also final values in line with reality. For this purpose, another reason that can push this price variation is the growing share of renewables connected to the grid. The variability of their production can be decisive for the energy price trends. In this section, a variation of 30% in the energy price between time bands is considered, the resulting values are:

- F1: 22.70 c€/kWh
- F2: 17.46 c€/kWh
- F3: 12.22 c€/kWh

The optimization results are reported in TABLE 6.

TABLE 6
TIME BAND SENSITIVITY ANALYSIS RESULTS.

Energy price variation	BESS charged during night?	NPV [€]	PV peak power [MW]	BESS capacity [MWh]
30%	No	28 674 885	1.62	1.54
	Yes	28 499 517	1.34	0.2

As supported by the NPV difference, charge the BESS during the night is not a suitable solution from an economic point of view. Despite a lower size of PV power plant and battery, which implies a lower installation cost, NPV in the second case is 175 k€ lower. It is important to understand the reasons of the unprofitability for this energy management system with these energy prices, three possible arguments are here reported:

- Number of cycles: as explained in Section II, the battery pack has a specific lifetime, corresponding to 3000 cycles, and then it needs to be replaced. With this approach, the BESS is charged and discharged more times in a day, increasing the daily number of cycles and so, increasing the number of replacements during the project lifetime.
- Charging and discharging efficiencies: this kind of storage system has a significant energy loss due to these efficiencies. Specifically, if 1 kWh is bought from the grid to charge the BESS, the resulting energy used for self-consumption is expressed in (8).

$$1\ kWh \cdot 0.96 \cdot 0.92 = 0.88\ kWh \tag{8}$$

- Presence of PV: the higher price time band, F1, starts at 8 a.m. when the PV production cover a part of the load and it is still increasing. It means that, for several days, the BESS cannot use all the energy stored during the night before the PV production overcomes the load curve. It will reduce the amount of solar energy stored increasing the energy surplus and worsening the economic profitability. For all these reasons, with whichever price variations between time bands, the best solution is to not charge the BESS during the night.

VI. CONCLUSION

This paper aims to find the optimal capacity of the PV and battery storage systems to be integrated inside an ultra-fast charging station for electric vehicles. The result of the optimization shows that the optimal solution consists in a system composed of a 1.30 MW photovoltaic power plant coupled with a 770-kWh BESS discharged with a rate of 0.5. This configuration allows a self-production of almost 50% out of the yearly energy required by the UFCS and, compared to the case in which all the energy is bought from the grid, the profitability increases by more than 2 million euros.

The NPV of the system is further increased in the sensitivity analysis, when the possibility to use a 4-hour BESS is considered; with this configuration, the NPV increases by 50 k€ even bringing a growth for PV and BESS sizes, respectively 1.38 MW and 900 kWh. In addition, the option to sell the surplus solar energy could be selected, as long as the amount of money earned is enough to cover the investment of a bidirectional converter that link the UFCS with the grid. On the other hand, charging the BESS during the night is not a viable strategy due to both economic and technical reasons.

By comparing the obtained results with those found in literature, the idea of coupling a PV power plant and a BESS for an UFCS

is widely supported indeed, in all the different optimization studies, it always brings economic savings from 10% up to 50%. To prove the effectiveness and computational time of the chosen optimization algorithm, it is compared with others found in literature and it can be concluded that the result accuracy and the convergence speed of GA is in line with other optimization algorithms. Therefore, it is feasible and effective to apply the GA algorithm to reach the optimal solution of the problem.

A possible future improvement for this work is represented by the exploitation of different renewable energy sources or different energy storage systems, that can be better solutions in different conditions or in other geographical areas. For example, a wind power plant could be coupled in the optimization algorithm to replace the PV plant, or integrated with it, according to the NPV maximization.

REFERENCES

[1] C. Liu, K. T. Chau, D. Wu, and S. Gao, "Opportunities and challenges of vehicle-to-home, vehicle-to-vehicle, and vehicle-to-grid technologies," *Proc. IEEE*, vol. 101, no. 11, pp. 2409–2427, 2013, doi: 10.1109/JPROC.2013.2271951.

[2] C. C. Chan, "The state of the art of electric, hybrid, and fuel cell vehicles," *Proc. IEEE*, vol. 95, no. 4, pp. 704–718, 2007, doi: 10.1109/JPROC.2007.892489.

[3] "• Italy: EV normal power charging points 2015-2020 | Statista." https://www.statista.com/statistics/906420/number-of-normal-power-charging-positions-in-italy/ (accessed May 25, 2021).

[4] H. Tu, H. Feng, S. Srdic, and S. Lukic, "Extreme Fast Charging of Electric Vehicles: A Technology Overview," *IEEE Trans. Transp. Electrif.*, vol. 5, no. 4, pp. 861–878, Dec. 2019, doi: 10.1109/TTE.2019.2958709.

[5] S. Deb, K. Tammi, K. Kalita, and P. Mahanta, "Impact of Electric Vehicle Charging Station Load on Distribution Network," *Energies 2018, Vol. 11, Page 178*, vol. 11, no. 1, p. 178, Jan. 2018, doi: 10.3390/EN11010178.

[6] L. Wang, Z. Qin, T. Slangen, P. Bauer, and T. van Wijk, "Grid Impact of Electric Vehicle Fast Charging Stations: Trends, Standards, Issues and Mitigation Measures - An Overview," *IEEE Open J. Power Electron.*, vol. 2, pp. 56–74, Jan. 2021, doi: 10.1109/OJPEL.2021.3054601.

[7] W. L. Liu, Y. J. Gong, W. N. Chen, Z. Liu, H. Wang, and J. Zhang, "Coordinated Charging Scheduling of Electric Vehicles: A Mixed-Variable Differential Evolution Approach," *IEEE Trans. Intell. Transp. Syst.*, vol. 21, no. 12, pp. 5094–5109, Dec. 2020, doi: 10.1109/TITS.2019.2948596.

[8] J. Hu, S. You, M. Lind, and J. Østergaard, "Coordinated charging of electric vehicles for congestion prevention in the distribution grid," *IEEE Trans. Smart Grid*, vol. 5, no. 2, pp. 703–711, Mar. 2014, doi: 10.1109/TSG.2013.2279007.

[9] C. Shao, T. Qian, Y. Wang, and X. Wang, "Coordinated Planning of Extreme Fast Charging Stations and Power Distribution Networks Considering On-Site Storage," *IEEE Trans. Intell. Transp. Syst.*, vol. 22, no. 1, pp. 493–504, Jan. 2021, doi: 10.1109/TITS.2020.3016765.

[10] M. S. Javed, A. Song, and T. Ma, "Techno-economic assessment of a stand-alone hybrid solar-wind-battery system for a remote island using genetic algorithm," *Energy*, vol. 176, pp. 704–717, Jun. 2019, doi: 10.1016/J.ENERGY.2019.03.131.

[11] W. Zhang, A. Maleki, M. A. Rosen, and J. Liu, "Sizing a stand-alone solar-wind-hydrogen energy system using weather forecasting and a hybrid search optimization algorithm," *Energy Convers. Manag.*, vol. 180, pp. 609–621, Jan. 2019, doi: 10.1016/J.ENCONMAN.2018.08.102.

[12] M. Moradzadeh and M. M. A. Abdelaziz, "A New MILP Formulation for Renewables and Energy Storage Integration in Fast Charging Stations," *IEEE Trans. Transp. Electrif.*, vol. 6, no. 1, pp. 181–198, Mar. 2020, doi: 10.1109/TTE.2020.2974179.

[13] J. Deng, J. Shi, Y. Liu, and Y. Tang, "Application of a hybrid energy storage system in the fast charging station of electric vehicles," *IET Gener. Transm. Distrib.*, vol. 10, no. 4, pp. 1092–1097, Mar. 2016, doi: 10.1049/IET-GTD.2015.0110.

[14] B. Sun, "A multi-objective optimization model for fast electric vehicle charging stations with wind, PV power and energy storage," *J. Clean. Prod.*, vol. 288, p. 125564, Mar. 2021, doi: 10.1016/J.JCLEPRO.2020.125564.

[15] J. A. Domínguez-Navarro, R. Dufo-López, J. M. Yusta-Loyo, J. S. Artal-Sevil, and J. L. Bernal-Agustín, "Design of an electric vehicle fast-charging station with integration of renewable energy and storage systems," *Int. J. Electr. Power Energy Syst.*, vol. 105, pp. 46–58, Feb. 2019, doi: 10.1016/J.IJEPES.2018.08.001.

[16] H. J. Vermaak and K. Kusakana, "Design of a photovoltaic–wind charging station for small electric Tuk–tuk in D.R.Congo," *Renew. Energy*, vol. 67, pp. 40–45, Jul. 2014, doi: 10.1016/J.RENENE.2013.11.019.

[17] K. Yunus, H. Z. De La Parra, and M. Reza, "Distribution grid impact of plug-in electric vehicles charging at fast charging stations using stochastic charging model," *Proc. 2011 14th Eur. Conf. Power Electron. Appl. EPE 2011*, 2011.

[18] H. Fathabadi, "Novel wind powered electric vehicle charging station with vehicle-to-grid (V2G) connection capability," *Energy Convers. Manag.*, vol. 136, pp. 229–239, Mar. 2017, doi: 10.1016/J.ENCONMAN.2016.12.045.

[19] O. Hafez and K. Bhattacharya, "Optimal design of electric vehicle charging stations considering various energy resources," *Renew. Energy*, vol. 107, pp. 576–589, Jul. 2017, doi: 10.1016/J.RENENE.2017.01.066.

[20] E. Mancini, M. Longo, W. Yaici, and D. Zaninelli, "Assessment of the Impact of Electric Vehicles on the Design and Effectiveness of Electric Distribution Grid with Distributed Generation," *Appl. Sci. 2020, Vol. 10, Page 5125*, vol. 10, no. 15, p. 5125, Jul. 2020, doi: 10.3390/APP10155125.

[21] S. M. Alshareef and W. G. Morsi, "Impact of fast charging stations on the voltage flicker in the electric power distribution systems," *2017 IEEE Electr. Power Energy Conf. EPEC 2017*, vol. 2017-October, pp. 1–6, Feb. 2018, doi: 10.1109/EPEC.2017.8286226.

[22] S. Bae and A. Kwasinski, "Spatial and temporal model of electric vehicle charging demand," *IEEE Trans. Smart Grid*, vol. 3, no. 1, pp. 394–403, Mar. 2012, doi: 10.1109/TSG.2011.2159278.

[23] Z. Zhou and T. Lin, "Spatial and temporal model for electric vehicle rapid charging demand," *2012 IEEE Veh. Power Propuls. Conf. VPPC 2012*, pp. 345–348, 2012, doi: 10.1109/VPPC.2012.6422675.

[24] G. Mauri and A. Valsecchi, "Fast charging stations for electric vehicle: The impact on the mv distribution grids of the milan metropolitan area," *2012 IEEE Int. Energy Conf. Exhib. ENERGYCON 2012*, pp. 1055–1059, 2012, doi: 10.1109/ENERGYCON.2012.6347725.

[25] C. Leone and M. Longo, "Modular Approach to Ultra-fast Charging Stations," *J. Electr. Eng. Technol.*, vol. 16, no. 4, pp. 1971–1984, Jul. 2021, doi: 10.1007/S42835-021-00757-X/FIGURES/19.

[26] K. Yunus, H. Z. De La Parra, and M. Reza, "Distribution grid impact of plug-in electric vehicles charging at fast charging stations using stochastic

charging model," *Proc. 2011 14th Eur. Conf. Power Electron. Appl. EPE 2011*, no. January 2011, 2011.

[27] "Report periodici delle singole stazioni | Anas S.p.A." https://www.stradeanas.it/it/le-strade/osservatorio-del-traffico/report-periodici-singole-stazioni (accessed May 03, 2021).

[28] "Italy: electric vehicle registrations by type 2018 | Statista." https://www.statista.com/statistics/1061823/electric-vehicle-registered-in-italy-by-type/ (accessed Nov. 29, 2021).

[29] C. Sabillon Antunez, J. F. Franco, M. J. Rider, and R. Romero, "A New Methodology for the Optimal Charging Coordination of Electric Vehicles Considering Vehicle-to-Grid Technology," *IEEE Trans. Sustain. Energy*, vol. 7, no. 2, pp. 596–607, Apr. 2016, doi: 10.1109/TSTE.2015.2505502.

[30] T. Boström, B. Babar, J. B. Hansen, and C. Good, "The pure PV-EV energy system – A conceptual study of a nationwide energy system based solely on photovoltaics and electric vehicles," *Smart Energy*, vol. 1, p. 100001, Feb. 2021, doi: 10.1016/J.SEGY.2021.100001.

[31] S. Funke, P. Jochem, S. Ried, and T. Gnann, "Fast charging stations with stationary batteries: A techno-economic comparison of fast charging along highways and in cities," *Transp. Res. Procedia*, vol. 48, pp. 3832–3849, Jan. 2020, doi: 10.1016/J.TRPRO.2020.08.036.

[32] K. Mongird, V. Viswanathan, J. Alam, C. Vartanian, V. Sprenkle, and R. Baxter, "2020 Grid Energy Storage Technology Cost and Performance Assessment," 2020.